Available online at www.sciencedirect.com
SCIENCE DIRECT®
Biochimica et Biophysica Acta 1608 (2004) 53–61
BIOCHIMICA ET BIOPHYSICA ACTA
BBA
www.bba-direct.com

Quantification of photosystem I and II in different parts of the thylakoid membrane from spinach

Ravi Danielsson, Per-Åke Albertsson, Fikret Mamedov, Stenbjörn Styring*

Department of Biochemistry, Center for Chemistry and Chemical Engineering, Lund University, P.O. Box 124, S-221 00 Lund, Sweden

Received 30 June 2003; received in revised form 23 September 2003; accepted 17 October 2003

Abstract

Electron paramagnetic resonance (EPR) was used to quantify Photosystem I (PSI) and PSII in vesicles originating from a series of well-defined but different domains of the thylakoid membrane in spinach prepared by non-detergent techniques. Thylakoids from spinach were fragmented by sonication and separated by aqueous polymer two-phase partitioning into vesicles originating from grana and stroma lamellae. The grana vesicles were further sonicated and separated into two vesicle preparations originating from the grana margins and the appressed domains of grana (the grana core), respectively. PSI and PSII were determined in the same samples from the maximal size of the EPR signal from $P700^+$ and $Y_D^\bullet$, respectively. The following PSI/PSII ratios were found: thylakoids, 1.13; grana vesicles, 0.43; grana core, 0.25; grana margins, 1.28; stroma lamellae 3.10. In a sub-fraction of the stroma lamellae, denoted Y-100, PSI was highly enriched and the PSI/PSII ratio was 13. The antenna size of the respective photosystems was calculated from the experimental data and the assumption that a PSII center in the stroma lamellae (PSIIβ) has an antenna size of 100 Chl. This gave the following results: PSI in grana margins (PSIα) 300, PSI (PSIβ) in stroma lamellae 214, PSII in grana core (PSIIα) 280. The results suggest that PSI in grana margins have two additional light-harvesting complex II (LHCII) trimers per reaction center compared to PSI in stroma lamellae, and that PSII in grana has four LHCII trimers per monomer compared to PSII in stroma lamellae. Calculation of the total chlorophyll associated with PSI and PSII, respectively, suggests that more chlorophyll (about 10%) is associated with PSI than with PSII.

Keywords: Photosystem I; Photosystem II; Thylakoid membrane; Photosystem antennae; EPR; Phase partition

1. Introduction

The light reaction of photosynthesis in higher plants is driven by the cooperation of two photosystems (PS), PSI and PSII, which, together with a chain of electron carriers, are localized in the photosynthetic membrane, the thylakoid [1]. This is differentiated into domains with characteristic biochemical composition and specialized function. From the geometry observed by electron microscopy, one can distinguish between appressed, planar domains of the grana and single paired membranes of the stroma lamellae connecting the grana; between the planar grana end membranes and the curved membranes of the grana margins. The quantification of the two photosystems in the different domains of the thylakoid membrane is of particular importance for our understanding of the function of the thylakoid membrane, how the two photosystems are co-coordinated during electron transport and how this is regulated.

Earlier studies, using fragmentation and separation analysis or immune electron microscopy, have shown that the two photosystems are segregated such that PSII is mainly localized in the appressed grana domain and PSI in the stroma exposed membranes, i.e. the stroma lamellae, end membranes and the grana margins (Fig. 1) [2–4]. The gross organization of PSII also differs and PSII dimers dominate in the grana and PSII monomers in the stroma-exposed membranes [5]. The two photosystems are also heterogeneous with respect to the size of their Chl-antenna system. One can distinguish between so-called PSIIα (large Chl antenna) in the grana and PSIIβ (small Chl antenna) in the stroma lamellae [6] and between PSIα (larger antenna) in

Abbreviations: Chl, chlorophyll (*a*+*b*); EPR, electron paramagnetic resonance; LHCII, light harvesting complex II; MES, 2-(*N*-morpholino) ethanesulfonic acid; P700, primary electron donor in PSI; PEG, polyethylene glycol; PSI, Photosystem I; PSII, Photosystem II; PpBQ, phenyl-*p*-benzoquinone; TEMPO, 2,2,6,6-tetramethyl-piperidinyloxy radical; Y_D, tyrosine D in PSII

* Corresponding author. Tel.: +46-46-222-01-08; fax: +46-46-222-45-34.
E-mail address: stenbjorn.styring@biokem.lu.se (S. Styring).

0005-2728/$ - see front matter © 2003 Elsevier B.V. All rights reserved.
doi:10.1016/j.bbabio.2003.10.005

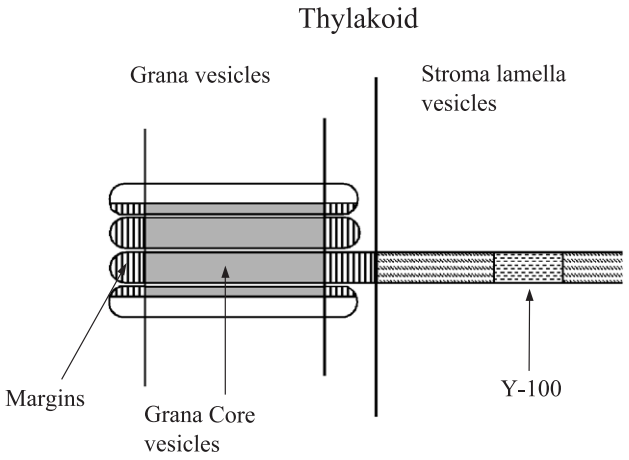

Fig. 1. Schematic representation of the different fractions of the thylakoid membrane isolated and analyzed in this study. The exact location of the Y-100 fraction is unclear, but it clearly represents a sub-domain in the stroma lamellae fraction.

the margins and PSIβ (smaller antenna) in the stroma lamellae and end membranes [7,8]. In addition, PSII is functionally very different in the different parts of the thylakoid membrane, probably reflecting an activity gradient due to the repair of PSII after photoinhibition [9].

Thus, the photosystems are not only laterally segregated in the thylakoid. They are also functionally segregated and photosynthetic electron flow in the different membrane compartments is likely to be very different. To a superficial extent (division in grana and stroma lamellae), this difference is quite well understood (see Refs. [2,4] and references therein). However, the thylakoid has more functionally distinct domains than the grana and stroma lamellae as is commonly thought. To fully understand the function of the dynamic thylakoid membrane, it is necessary to have a detailed knowledge both about the function of the two photosystems and their relative abundance in the different domains of the thylakoid. We have earlier presented a functional analysis of PSII in the different thylakoid domains [9]. The dominating part of PSII in the grana region has a functional acceptor side and an active oxygen-evolving complex. In contrast, large part of PSII in the stromal region is inactive on either or both the acceptor and donor sides. Several other pools of PSII with more inhomogeneous function are also found both in the stroma lamellae and the margins of the grana [9].

The aim of the present study is to quantify, with precision, the two photosystems versus each other (determine the PSI/PSII ratio) not only in the whole thylakoid but also in each of the different sub-thylakoid fractions. To this end, we have fragmented the thylakoid membrane and isolated vesicles originating from different parts of the membrane. The two photosystems have then been quantified by using electron paramagnetic resonance (EPR) spectroscopy, which is a more robust and precise method for this purpose than earlier applied methods.

2. Materials and methods

2.1. Preparation of thylakoid membranes

Spinach (*Spinachia oleracia* L.) was grown hydroponically under cool white fluorescent light at 20 °C with light–dark periods of 12 h and with the light intensity of 300 μE m^{-2} s^{-1}. Two-month-old plants were dark-adapted 24 h before harvesting to reduce the content of starch grains. All preparation procedures were made in weak green light at 4 °C, and the sample was kept on ice through the whole process. The thylakoid membranes were prepared with a medium containing 5 mM $MgCl_2$, as in Ref. [7], and resuspended in 10 mM sodium phosphate buffer pH 7.4, 5 mM NaCl, 1 mM $MgCl_2$ and 100 mM sucrose to a chlorophyll concentration of 3–4 mg/ml. This buffer was used for the sub-fractionation purifications. For EPR measurements, the thylakoids and the sub-thylakoid fractions were washed once and then dissolved to high Chl concentration in 15 mM 2-(*N*-morpholino) ethanesulfonic acid (MES) pH 6.5, 15 mM NaCl and 300 mM sucrose. All sub-thylakoid fractions were frozen after preparation and stored at −80 °C.

2.1.1. Preparation of grana and stroma lamella vesicles

Thylakoid membrane suspension (8.2 g, at 3–4 mg Chl/ml) was added to 32.8 g of a polymer mixture to give the final concentrations: 5.7% (w/w) $Dextran^{500}$, 5.7% (w/w) polyethylene glycol $(PEG)^{4000}$, 10 mM sodium phosphate buffer pH 7.4, 3 mM NaCl, 1 mM $MgCl_2$ and 20 mM sucrose. The thylakoid-polymer suspension was then sonicated by a Vibra-cell ultrasonic processor Model VC 500 (Sonics and Materials, Danbury, CT, USA) equipped with a 3/4-in. horn. The sample was sonicated 8 × 30 s, with 1-min resting intervals in a cylindrical aluminium tube which was cooled in ice water. The temperature was controlled never to exceed 6 °C. The ultrasonic exposure had an intensity output setting of 7, with 20% duty pulse. This sonication procedure breaks the thylakoids into two main domains, grana vesicles and stroma lamellae vesicles (Fig. 1) [7]. To the sonicated mixture was added 10 g of pure bottom phase and 10 g of pure top phase from an aqueous two-phase system, composed of 5.7% (w/w) $Dextran^{500}$, 5.7% (w/w) PEG^{4000}, 10 mM sodium phosphate buffer pH 7.4, 5 mM NaCl and 20 mM sucrose. The two-phase system (at 4 °C) was shaken, mixed and centrifuged at 2000 × *g* for 6 min to separate the phases. The top phase (T1) was carefully collected and a thin layer above the interface was left. This leftover, together with the interface and the bottom phase, is here named the bottom phase fraction (B1). Fresh bottom phase (23 ml) was added to the T1 fraction and 23 ml fresh top phase to the B1 fraction. Each phase system was treated as above. In this way, a top phase fraction (T2) is obtained from the T1 fraction and a bottom phase fraction (B2) from the B1 fraction. This procedure is repeated, giving the final T3 and B3 fractions.

The resulting top phase fraction, denoted T3, originating mainly from stroma lamella and end membranes, and the bottom phase fraction denoted B3, originating from appressed regions and margins of the grana (Fig. 1) [7] were diluted three times with 15 mM MES pH 6.5, 15 mM NaCl and 300 mM sucrose. They were then centrifuged at 100 000 × g for 120 min. The pellets were resuspended in the same buffer to a chlorophyll concentration of approximately 1.5–2.5 mg/ml.

2.1.2. Preparation of grana core and margin vesicles

Isolation of grana core vesicles and margins was carried out by sonicating (20 × 30 s with output 9) the bottom phase fraction B3 (see above) containing the grana vesicles. The resulting fragments were separated by two-phase partitioning, in exactly the same manner as described above, to yield new top and bottom phase fractions containing vesicles originating from the margin and the grana core, respectively (Fig. 1) [10].

2.1.3. Preparation of Y-100 vesicles

For preparation of Y-100 particles (Fig. 1), isolated thylakoid membranes (2–3 mg Chl/ml) in a buffer solution composed of 10 mM sodium phosphate pH 7.4, 5 mM NaCl, 5 mM $MgCl_2$ and 100 mM sucrose were twice passed through a Yeda press at 4 °C and at a nitrogen pressure of 10 MPa [3,11,12]. The Yeda press homogenate was diluted five times with the same buffer but without $MgCl_2$ and centrifuged at 40 000 × *g* at 4 °C for 30 min. The membrane vesicles in the supernatant were sedimented by centrifugation at 100 000 × *g* at 4 °C for 60 min to yield the Y-100 vesicles. The last pellet was resuspended in 15 mM MES pH 6.5, 15 mM NaCl and 300 mM sucrose to 1.5–2.5 mg Chl/ml.

2.2. Characterization of the sub-thylakoid fractions

The chlorophyll concentration was determined according to Arnon [13] to allow a comparison with earlier work where the Arnon method was used. For values of total chlorophyll (*a* + *b*) the values obtained by the Arnon method could be multiplied by a factor of 0.895 to obtain corresponding values by the method of Porra et al. [14]. Steady state oxygen evolution was measured with a Clark electrode at 20 °C using saturating white light. The sample concentration was 20 μg Chl/ml, and 2 mM ferricyanide and 0.5 mM phenyl-*p*-benzoquinone (PpBQ) were used as electron acceptors. The measurements were done in 15 mM MES pH 6.5, 15 mM NaCl and 300 mM sucrose.

2.3. EPR measurements and analysis

Room temperature EPR was measured with a Bruker Elexys E500 spectrometer equipped with a standard Bruker 4102 cavity. A flat cell with 250 μl volume was used. The relative amount of PSI in the different fractions was estimated on the basis of the intensity of non-saturated EPR spectra from chemically oxidized $P700^+$. $P700^+$ amounts to one radical per functional PSI center and is independent of the antenna size. P700 was oxidized in the dark at 20 °C using 5 mM ferricyanide for 10 min. This concentration and incubation time was found to induce maximal size of $P700^+$ in all fractions (not shown). Lower concentrations of ferricyanide and/or shorter incubation times gave incomplete $P700^+$ formation.

The relative amounts of PSII in the different fractions were estimated on the basis of the intensity of the non-saturated EPR spectra from the dark stable radical from $Tyrosine_D$, $Y_D^\bullet$. When properly photoinduced, there is one $Y_D^\bullet$ radical in each functional PSII center and this does not depend on the antenna size, the presence of the Mn-cluster or the electron transfer between Q_A and Q_B [15–17]. Full induction of $Y_D^\bullet$ was accomplished by 30-s illumination of the sample in room light at 20 °C, followed by 5 min dark incubation prior to the measurement [18]. This procedure was found to result in maximal signal from $Y_D^\bullet$ in all fractions investigated, despite the widely varying antenna size of PSII.

The spectral intensities of the $Y_D^\bullet$ and $P700^+$ spectra were determined by double integration of the spectra.

2.4. Determinations of chlorophyll per reaction center

Exact quantification of concentrations of a radical species by means of EPR was achieved by comparison with the EPR spectrum from a spin probe with known concentrations, for instance 2,2,6,6-tetramethyl-piperidinyloxy radical (TEMPO). The area of the EPR spectrum from the known spin probe was compared with the areas of the EPR spectra from the radical species under investigation.

In our case, the calculations of concentrations of the reaction centers for PSII ($Y_D^\bullet$) and PSI ($P700^+$) were based on a standard calibration curve made with the well-known, often used radical standard TEMPO. The measurements for TEMPO were performed with the same EPR parameters as for the sub-thylakoid fractions (see Fig. 2) using eight different concentrations of TEMPO between 0.391 and 100 μM. By plotting the double-integrated areas from the spectra recorded at the different concentrations of TEMPO, a standard curve was obtained (not shown). This standard curve was used to determine the exact concentration of PSII ($Y_D^\bullet$) and PSI ($P700^+$) radicals in the different fractions by using the double-integrated areas from their EPR spectra.

3. Results

3.1. Characterization of thylakoid membrane and sub-thylakoid fractions

A general account of the procedure and characterization of the different sub-thylakoid vesicle fractions has been

published [19]. Table 1 summarizes the oxygen evolution and the Chl *a*/*b* ratios in the different fractions. In essence, our results agree with the results in earlier studies [9,19]. The highest oxygen evolution (on Chl basis) was found in the grana core vesicles. It was less in the grana and still less in the margin and the stroma lamellae vesicles. There was (on Chl basis) nearly no detectable oxygen evolution in the Y-100 sub-fraction.

3.2. Determination of the relative amounts of PSII and PSI in the thylakoid sub-fractions

Our target is to use highly resolving spectroscopic techniques to quantify the large photosynthetic redox enzymes in the different compartments of the highly dynamic thylakoid membrane. Here we study PSI and PSII, for which EPR spectroscopy is a particularly useful technique since both photosystems can be very accurately quantified by extremely well-characterized radicals in their respective reaction centers.

3.2.1. EPR measurement of $Y_D^\bullet$ in the thylakoid and sub-thylakoid fractions

We have chosen to quantify PSII by using the dark stable radical EPR signal from $Y_D^\bullet$. The $Y_D^\bullet$ radical originates from the neutral radical form of Y-161 on the D2 protein in spinach [20,21]. Since it originates from a defined amino acid, the yield of the radical can never exceed one radical per PSII reaction center. The $Y_D^\bullet$ radical is also extremely stable and the radical life time is tens of minutes to many hours depending on S-state and material [17,18,22–24]. The radical is efficiently induced by illumination and can, due to its long lifetime, be measured quite easily and very accurately.

Fig. 2 shows the EPR spectra of $Y_D^\bullet$ in the intact thylakoid membranes and the different sub-fractions. All spectra shown are normalized to the same Chl concentration to allow easy comparison. The spectra are recorded in samples which were first illuminated for 30 s, then dark-adapted for 5 min. This treatment is known to result in complete oxidation of $Y_D^\bullet$ in active and photoactivating PSII centers [16,22]. We also tested this (not shown) and found this illumination region to allow quantitative induction of $Y_D^\bullet$ in all fractions. Severely photoinhibited PSII centers are inactive in forming $Y_D^\bullet$ [25,26].

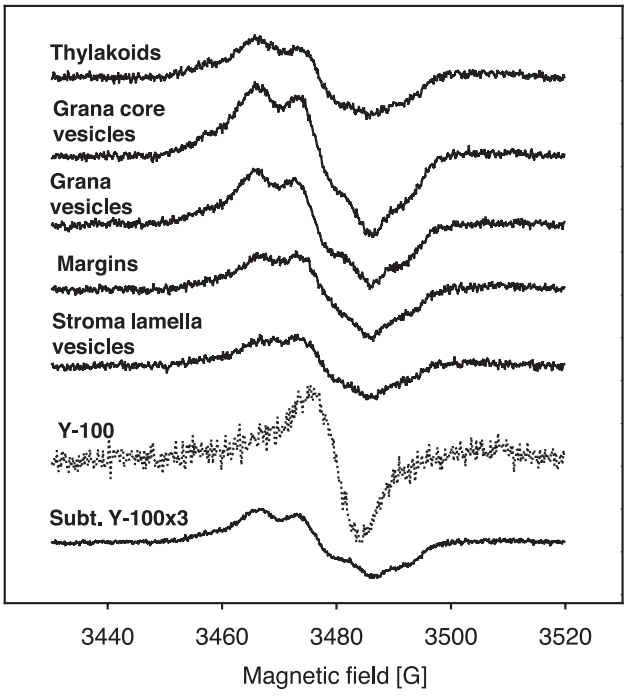

Fig. 2. EPR spectra (recorded in the dark after illumination that fully oxidize $Y_D^\bullet$ (see Section 2) of $Y_D^\bullet$ from PSII in different fractions of the thylakoid membrane. The spectra are normalized to the same Chl concentration. The spectrum from the Y-100 fraction (dotted curve) is a mixture of the signal from $Y_D^\bullet$ and a radical of unknown origin (see text). A pure spectrum of $Y_D^\bullet$ was weighted out from the mixed spectrum to allow quantification of $Y_D^\bullet$. The full drawn curve shows the pure $Y_D^\bullet$ spectrum (multiplied by a factor of 3) that was weighted out from the Y-100 spectrum and that was used for quantification (see text). EPR conditions: temperature 293 K; microwave frequency 9.76 GHz; microwave power 8 mW; modulation amplitude 5 G.

Table 1
Characterization of the different fractions of the thylakoid membrane

Fraction (Fig. 1)	Number of preparations analyzed	Chl *a*/*b* (mol/mol)	O_2 evolution (μmol of O_2 (mg of Chl)$^{-1}$ h^{-1})
Thylakoid	5	3.08 ± 0.06	125 ± 5
Grana core vesicles	3	2.23 ± 0.06	271 ± 16
Grana vesicles	3	2.41 ± 0.04	249 ± 26
Margins	3	2.90 ± 0.11	90 ± 10
Stroma lamella vesicles	3	4.61 ± 0.02	78 ± 4
Stroma lamella vesicles (Y-100)	3	7.11 ± 0.25	25 ± 7

In the thylakoid and grana preparations, the shape of the EPR spectrum is entirely dominated by $Y_D^\bullet$ [17,22]. In the margins, stroma lamellae and the Y-100 fractions the EPR spectra are different and the peak at 3473 G is somewhat higher than the left shoulder at 3466 G. The left shoulder originates entirely from $Y_D^\bullet$ while the middle peak contains both $Y_D^\bullet$ and a non-structured, narrow free radical spectrum from another species than PSII. The radical that gives rise to the narrow unstructured spectrum in the margins, stroma lamellae and Y-100 fractions is very stable and has EPR properties similar to $P700^+$ (7.5–8.5 G wide, $g = 2.0026$) [17]. It could consequently reflect a minor, abnormally stable fraction of $P700^+$. However, it should also be made clear that the exact origin of this non-PSII radical does not interfere with our determination of the PSII content in the fraction. In the margins and stroma lamellae, this non-PSII radical only amounts to a few percent and could easily be subtracted from the spectrum. In contrast, it is significantly bigger in the spectrum from the Y-100 fraction, where

it needed careful treatment in our analysis (see below). Fig. 2 shows that the signal from $Y_D^{\bullet}$ is largest (on a Chl basis) in the grana preparation and smaller in the stroma lamellae compared to the intact thylakoid membranes. The signal in the margin preparation is also smaller than in the grana fractions while the spectrum is very small in the Y-100 fraction ($Y_D^{\bullet}$ is the very small shoulder at 3466 G in the dotted spectrum).

To obtain "clean" spectra of $Y_D^{\bullet}$ in the margins and stroma lamella fractions, we first had to subtract the radical contamination from the spectra in Fig. 2. This was done by subtractions of a suitable amount of a narrow radical spectrum to arrive at a pure spectrum from $Y_D^{\bullet}$. The subtraction never exceeded a few percent (4–8%) of the total spectrum. The purity of the resulting spectrum from $Y_D^{\bullet}$ (not shown) was ascertained by overlapping with the clean $Y_D^{\bullet}$ spectrum recorded in the grana core fraction.

Table 2 shows the quantitative analysis obtained from double integration of the spectra. The relative PSII concentration is almost three times higher in the core of the grana stacks than in the stroma lamellae. The margin preparations are clearly of an intermediate character, having a much lower PSII concentration than the grana preparations. Consequently, the grana vesicles that contain both the margins and the grana core (Fig. 1) are intermediate in PSII concentration between these two fractions.

The spectrum recorded from the Y-100 fraction (Fig. 2, dotted line) was clearly a mixed spectrum from a small $Y_D^{\bullet}$ radical (visible as a small shoulder at 3466 G) and a larger (in relative size) radical spectrum in the middle part of the spectrum. Therefore, $Y_D^{\bullet}$ could not be quantified directly. Since the spectrum from the unknown radical (may be reflecting a tiny fraction of stable $P700^+$, see above) in these fractions was of equal size or even larger than the $Y_D^{\bullet}$ spectrum, it was almost impossible to subtract this away from the recorded spectrum (Fig. 2, dotted spectrum). Instead, we used a pure spectrum from $Y_D^{\bullet}$ (recorded in the grana core fraction) to completely subtract away the $Y_D^{\bullet}$-shoulder in the spectrum from the Y-100 fraction. In that way, we obtained a pure spectrum from the unknown radical. The concentration of $Y_D^{\bullet}$, in turn, was estimated from the intensity of the $Y_D^{\bullet}$ spectrum needed to completely subtract $Y_D^{\bullet}$ away from the original spectrum. This is shown as the full drawn spectrum from the Y-100 fraction in Fig. 2 (note that this spectrum is magnified three times). This analysis reveals that the relative concentration of PSII (on a Chl basis) in the Y-100 fraction is ca. 23% and 13% of that in the starting thylakoid fraction and the grana core, respectively (Table 2).

To conclude, most of the PSII is found in the granal part of the membrane. The largest concentration of PSII on a Chl basis is found in the grana core and then it decreases in the other fractions. Compared with Y-100, there are 7.4 and 6.5 times stronger signals from PSII in the grana core and grana, respectively (on a Chl basis). The signals are intermediate in the thylakoid and the margins, 4.5 and 4.1 times stronger, respectively, and 2.7 times stronger in stroma lamella than in Y-100.

Table 2
Quantification of PSI and PSII in different fractions of the thylakoid membrane

Fraction of thylakoid membrane (Fig. 1)	Number of preparations analyzed	$P700^{+a}$ (arb. units)	$Y_D^{\bullet b}$ (arb. units)	PSI/PSII[c]
Entire thylakoid	5	35.3 ± 2.2	31.8 ± 2.6	1.13 ± 0.05
Grana core vesicles	3	15.4 ± 1.4	53.9 ± 2.8	0.25 ± 0.06
Grana vesicles	3	19.7 ± 1.0	47.3 ± 4.3	0.43 ± 0.05
Margins	3	38.1 ± 0.6	30.1 ± 3.4	1.28 ± 0.14
Stroma lamella vesicles	3	61.3 ± 1.7	20.0 ± 0.4	3.10 ± 0.11
Stroma lamella vesicles (Y-100)	3	87.8 ± 3.1	7.3 ± 1.1	12.75 ± 1.65

[a] Determined from the maximal intensity of $P700^+$ determined by double integration the $P700^+$ EPR spectra. The data are normalized to the same Chl concentration as for PSII.

[b] Determined from the maximal intensity of $Y_D^{\bullet}$ determined by double integration the $Y_D^{\bullet}$ EPR spectra. The data are normalized to the same Chl concentration as for PSI.

[c] The values of PSI/PSII shown are not exactly the ratio of the numbers from the $P700^+$ and $Y_D^{\bullet}$ columns in the table. Instead, the reported values represent the means of the ratio of $P700^+$ and $Y_D^{\bullet}$ obtained from each independent preparation analyzed.

3.2.2. EPR measurements of $P700^+$ in the thylakoid and sub-thylakoid fractions

The PSI concentration was analyzed in an analogous manner as for PSII. In this case, we used the EPR signal from the $P700^+$ radical, recorded in samples oxidized with ferricyanide, to estimate PSI. Also, $P700^+$ maximally amounts to one radical per PSI reaction center. However, it is possible that oxidation with ferricyanide is incomplete in some fractions. We therefore tested this, and 10 min incubation with 5 mM ferricyanide was found to induce maximal $P700^+$ signals in all fractions studied (not shown). Shorter incubation or lower concentration of the oxidant failed to be complete, while higher concentration of ferricyanide and/or longer incubation times did not increase the yield of $P700^+$.

The spectra from the ferricyanide-oxidized samples are shown in Fig. 3A. These EPR spectra contain a mixture of the stable signal from $Y_D^{\bullet}$ and the signal from $P700^+$. The $Y_D^{\bullet}$ contribution to the spectra is clearly observed as a shoulder at 3466 G in the spectra from the grana, margins, and thylakoids (Fig. 3A) and it is also present in the other spectra albeit to a lower, less obvious extent. In order to determine the contribution from $P700^+$ only, the spectra of $Y_D^{\bullet}$ (Fig. 2) were subtracted from the spectra in Fig. 3A. This resulted in the difference spectra displayed in Fig. 3B. From these, the concentration of $P700^+$ could be estimated and the results are presented in Table 2. The smallest signal

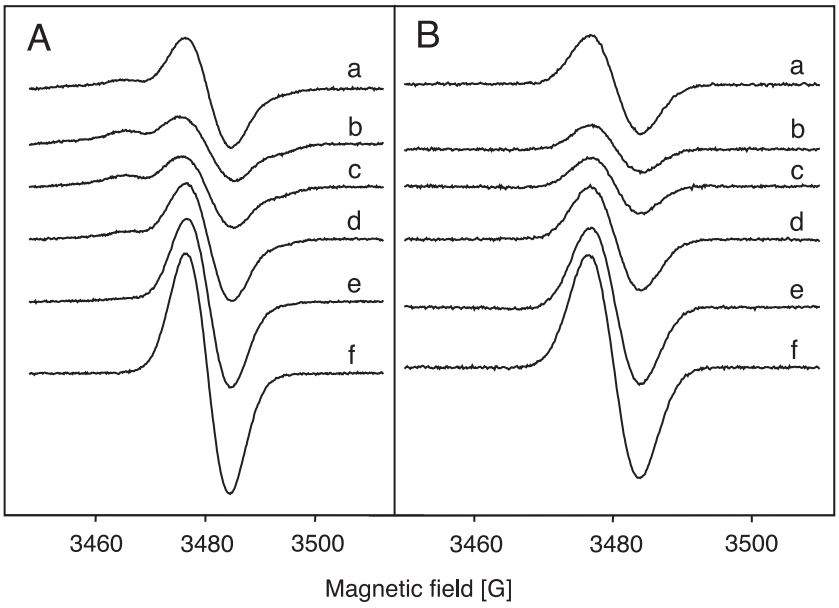

Fig. 3. (A) EPR spectra recorded in the different thylakoid fractions after oxidation with 5 mM ferricyanide in the dark for 10 min. The spectra originate from a mixture of $P700^+$ from PSI and $Y_D^\bullet$ from PSII. The contribution from $Y_D^\bullet$ is clearly seen as a shoulder at 3466 G in for example the thylakoid fraction. (B) EPR difference spectra of 5 mM ferricyanide oxidized (spectra in panel A) minus dark (spectra in Fig. 2) showing the pure $P700^+$ spectrum from the different fractions of the thylakoid membrane. Both panels show spectra taken from: (a) thylakoids; (b) the grana core fraction; (c) the grana fraction; (d) the margin fraction; (e) the stroma lamellae fraction; (f) the Y-100 fraction. The EPR conditions are the same as in Fig. 2.

from $P700^+$ (Fig. 3B) was found in the grana core (Table 2) while PSI completely dominated the stromal fractions. The signals are 5.7 and 4.4 times smaller (on a Chl basis) in grana core and grana, respectively, compared to the Y-100 vesicles. In the thylakoids and the margins, the relative PSI concentration is intermediate, 2.5 and 2.3 times smaller, respectively, than in the Y-100 vesicles. The $P700^+$ signal in stroma lamellae is 1.4 times smaller than in the Y-100 vesicles. It should also be noted that our analysis in the Y-100 fraction provides a number for $P700^+$ which includes both the dark stable radical (ca. 7–8% of total $P700^+$) and the ferricyanide-oxidized $P700^+$.

3.3. PSI/PSII ratio in the thylakoid and sub-thylakoid fractions

The data obtained from integration of the EPR spectra of $Y_D^\bullet$ (Fig. 2) and $P700^+$ (Fig. 3B) directly allow determination of the PSI/PSII ratio in the different fractions with high accuracy, simply by comparing the double-integrated area of the spectra. The results are shown in Table 2. In the intact thylakoid membranes, we find a PSI/PSII ratio of 1.13 ± 0.05. Thus, in our spinach leaves, there are slightly more PSI than PSII centers. However, they are very unevenly distributed in the membrane. PSI dominates in the stroma lamellae (PSI/PSII is 3.10 ± 0.20) and dominates even further in the Y-100 fraction (PSI/PSII is 12.75 ± 1.65). Thus, patches seems to exist in the membrane where PSII is almost absent. In contrast, PSII is more abundant than PSI in the grana and PSI/PSII is 0.25 ± 0.06 in the grana core fraction, which is the purest PSII fraction we obtained with our fractionation procedure. In the margins, there is a little more PSI than PSII (PSI/PSII is 1.28 ± 0.13).

It should be emphasized that the overall picture we find here is not new. It has been known for decades that PSII is enriched in the grana, PSI in the stroma lamellae [2,3], and more recent studies have shown that both PSI and PSII are present in margins preparations [10]. However, our quantification using EPR, which allows direct comparison of PSII and PSI by the same measurement, is novel and the PSI/PSII ratios we describe here are probably the most accurate so far determined.

3.4. Concentration of PSI and PSII reaction center per chlorophyll

With EPR spectroscopy, the concentration of a radical species can be determined very accurately by comparison with the EPR spectrum from a radical with known concentration. Such spin quantification is not dependent on properties like light scattering, overlapping of optical absorption from other species, difficult determination of extinction coefficients, fluorescence yield, etc., which are inherent for all optical spectroscopy and fluorescence measurements in photosynthetic membranes.

We determined the concentration on a Chl basis of the $Y_D^\bullet$ (Fig. 2) and $P700^+$ (Fig. 3B) radicals in the different preparations by comparison with a standard calibration curve from TEMPO, an often used spin probe [27]. The data are presented on a Chl basis in Table 3. Table 3 also presents the number of Chl molecules per PSI or PSII reaction center in each fraction. This is useful for the

Table 3
Chlorophyll molecules per reaction center on the basis of $Y_D^{\bullet}$ (PSII) and $P700^+$ (PSI) in different domains of the thylakoid membrane

Fraction (Fig. 1)	$Y_D^{\bullet}$ [a] (mol/1000 mol Chl)[b]	Chl/$Y_D^{\bullet}$ [c]	$P700^+$ [a] (mol/1000 mol Chl)[b]	Chl/$P700^+$ [c] (mol/mol)
Thylakoid	1.62	617	1.81	552
Grana core vesicles	2.82	355	0.77	1300
Grana vesicles	2.45	408	1.02	980
Margins	1.50	667	1.97	508
Stroma lamella vesicles	1.03	971	3.16	316
Stroma lamella vesicles (Y-100)	0.36	2780	4.50	222

All data are average values of three or five measurements.
[a] The absolute concentrations of $Y_D^{\bullet}$ and $P700^+$ were determined from a standard spin concentration curve using TEMPO as a spin standard.
[b] Chl *a* + Chl *b*.
[c] Total number of Chl molecules (*a* + *b*) per PSII or PSI center. Note that all these chlorophylls are not connected to PSII or PSI (see Section 4 for explanation of the calculation of antenna size).

calculation of the antenna size of the two photosystems, see below, Section 4.2.

4. Discussion

4.1. PSI/PSII ratios

The overall relative distribution of PSI and PSII between the different fractions agrees with what one would expect from earlier studies using fragmentation and separation analysis [2,19]. However, the absolute values from our determination of PSII differ from other results obtained with other techniques. Our data give lower PSII concentrations and hence larger PSI/PSII ratios than previously reported in the literature. Thus, we find for whole thylakoids a PSI/PSII ratio of 1.13 while most other studies report values in the range of 0.5–0.9 [11,28–35].

In the case of PSI, its reaction center, P700, has been determined by difference absorption of the oxidized minus reduced form at 705 nm using an absorption coefficient determined by Hiyama and Ke [36]. There seems to be consensus with regard to the determination of PSI. Our results also agree with earlier published values for Chl/P700. Thus, for the Y-100 fraction, we obtain a value of 222 Chl/P700 (Table 3) compared to 210–240 obtained by using light microscopy [11,37,38].

In the case of PSII, the situation is more complicated and controversial. Optical spectroscopy has been used for quantification of the reduced primary quinone acceptor Q_A [11,28–30,35] and pheophytin [30]. Flash oxygen yield [32,35], and flash-induced proton release measurements [33] have also been used. The results obtained from these different assays are variable, leading to reported PSI/PSII ratios of 0.5–0.9. Binding studies of atrazin to thylakoids have also given variable PSI/PSII ratios such as 0.6 [31,35] or 1.0 [39]. The discrepancies can only partly be explained by varying plant material and growth conditions. It is known that light conditions influence the PSI/PSII ratio [31], but even for spinach grown under fairly similar conditions and for which the Chl *a*/*b* ratios are the same, the results differ. In sum, several earlier studies report varying PSI/PSII ratios which are less than 1 as compared to our value which is slightly larger than 1.

It is not unlikely that reported differences in the PSI/PSII ratio also might reflect non-functional PSII centers, which do not appear in the conventional assays [40]. We don't wish to speculate on the origin of discrepancies with earlier reports but argue that EPR is a more robust method to determine the concentrations of PSI and PSII, since the signals measured are only dependent on the number of spins and not on the complete activity of the centers. In addition, the signals from both PSI and PSII are determined in the same sample. Our data are supported by the calculation of the antenna size which agrees with what one would expect from analysis of protein composition of the two photosystems, see below.

4.2. Calculation of the antennae size

The fractionation scheme gives two types of vesicles, which are highly enriched: Y-100 (stroma lamellae) in PSI and another, grana core vesicles, in PSII. Therefore, our data allowed calculation of the antenna size of the two photosystems in the following way.

For each vesicle preparation, the following balance equation holds:

$$N_{tot} = n_I N_I + n_{II} N_{II} \quad (1)$$

where n_I and n_{II} are the number of reaction centers of PSI and PSII, respectively, and N_I and N_{II} are the average number of Chls in their respective antennae. N_{tot} is the total number of Chls in the preparation.

For the antennae of PSI:

$$N_I = \frac{N_{tot}}{n_I} - \left(\frac{n_{II}}{n_I} \times N_{II}\right) \quad (2)$$

For the most PSI-enriched (stroma lamellae) preparation, Y-100 $N_{tot}/n_I = 222$ (Table 3), $n_{II}/n_I = 0.078$ (Table 2). In this preparation, PSII is in the form of the so-called β-centers which have a small antennae [6,28]. The number of antenna Chl per PSII center in PSIIβ can be assigned a value of approximately 100 Chl/PSII center based on PSII lacking light-harvesting complex II (LHCII) [40] (see also below). Inserting these values in Eq. (2), a value of $N_I = 214$ for the average antennae size of PSI in the stroma lamellae (N_I for PSIβ) is obtained.[1]

[1] It should be noted that the assigned antenna size of PSIIβ does not significantly affect the value of N_I since the concentration of PSIIβ is so low in the Y-100 fraction. For example, if we instead assign a value of 50 Chl/PSIIβ the N_I value would only change to 218.

It is known from earlier studies [8,37] that the antennae size of PSI in the grana (N_I for PSIα) is about 40% larger, i.e. 300. That the antennae of PSI in the grana (PSIα) is larger than PSI in the stroma lamellae (PSIβ) is a result of attachment of LHCII trimers (Lhcb,1,2) to PSIβ. If it is assumed that one LHCII monomer contains 15 Chl, the data fit a model where two LHCII trimers (=90 Chl) are attached to PSI in the grana (PSIα) [41].

For the antennae size of PSII:

$$N_{II} = \frac{N_{tot}}{n_{II}} - \left(\frac{n_I}{n_{II}} \times N_I\right) \quad (3)$$

For the most PSII-enriched preparation, the grana core vesicles, $N_{tot}/n_{II} = 355$ (Table 3), $n_I/n_{II} = 0.25$ (Table 2), $N_I = 300$ (see above). Inserting these values in Eq. (3), gives a value of $N_{II} = 280$ for the antennae size of PSII in the grana core (N_{II} for PSIIα).

A similar calculation applied to the grana vesicles results in an average antennae size of (N_{II}) 279 Chls per PSII monomer and for margins this value will be 283. This points to a fairly homogeneous distribution of the antenna size of PSII over the grana disc. The antenna size of the PSII core without any attached LHC proteins is about 50 Chls [42,43]. Together with the minor light-harvesting polypeptides (Lhcb,4,5,6) the antenna size of PSII monomer without any LHCII trimers attached can be assigned a value of about 100 Chl [41]. Thus, our determined antenna size of 280 Chls/PSII center indicates that there are about four LHC trimers per PSII monomer in the granal part of the membrane. Since PSII in grana is dimeric [5] it means eight LHCII trimers per dimer. This supports earlier models presented for PSII based on biochemical fractionation after mild detergent treatment [41,44–46] and is also compatible with models suggested from transmission electron microscopy [5,47].

4.3. The overall distribution of total chlorophyll between PSI and PSII in the thylakoid membranes

It has been shown earlier that mild sonication followed by counter-current distribution can fractionate the thylakoid membrane quantitatively into two, well-separated populations of membrane vesicles denoted α and β vesicles [7]. The α-vesicles originate from the grana and the β-vesicles from the stroma lamellae and the end membrane: 36% and 64% of P700 are found in the α- and β-vesicles, respectively, and about 80% and 20% of PSII are found in the α- and β-vesicles, respectively [2,7]. In the literature, values between 15% and 35% of the total PSII centers are assigned to PSIIβ [6,28,29]. If we combine these data with the values for the antennae of the respective photosystems calculated above, the overall distribution of Chl associated with PSI and PSII, respectively, can be calculated as follows:

$$\frac{N_{Itot}}{N_{IItot}} = R \times \frac{(p_I N_{I\alpha} + q_I N_{I\beta})}{(p_{II} N_{II\alpha} + q_{II} N_{II\beta})} \quad (4)$$

where R is the PSI/PSII reaction center ratio of the thylakoid; p_I and q_I are the fractions of PSI reaction centers in the (α) and (β) vesicles, respectively, ($p_I + q_I = 1$); p_{II} and q_{II} are the corresponding fractions for PSII. Inserting the values $R = 1.13$, $p_I = 0.36$ and $q_I = 0.64$ and $p_{II} = 0.8$ and $q_{II} = 0.2$, $N_{I\alpha} = 300$, $N_{I\beta} = 214$, $N_{II\alpha} = 280$ and $N_{II\beta} = 100$ in Eq. (4) gives a value of 1.1 for N_{Itot}/N_{IItot}, i.e. in the thylakoid membrane from our spinach more Chl is associated with PSI than PSII. Since carotenoids distribute in a similar fashion as Chl between different sub-thylakoid vesicles [48] one can conclude that more pigments are associated with PSI. This agrees with earlier fractionation studies [2,4,39] and with action spectra which demonstrate that PSI captures more quanta than PSII [49,50].

Acknowledgements

This work was supported by The Swedish Research Council, The Swedish National Energy Administration, DESS, and the Knut and Alice Wallenberg Foundation.

References

[1] R.E. Blankenship, Molecular Mechanisms of Photosynthesis, Blackwell, Oxford, 2002.
[2] P.-Å. Albertsson, A quantitative model of the domain structure of the photosynthetic membrane, Trends Plant Sci. 6 (2001) 349–354.
[3] B. Andersson, J.-M. Anderson, Lateral heterogeneity in the distribution of chlorophyll–protein complexes of the thylakoid membranes of spinach chloroplasts, Biochim. Biophys. Acta 593 (1980) 427–440.
[4] P.-Å. Albertsson, The domain structure and function of the thylakoid membrane, Recent Res. Dev. Bioenerg. 1 (2000) 143–171.
[5] J. Barber, Photosystem II: a multisubunit membrane protein that oxidases water, Curr. Opin. Struck. Biol. 12 (2002) 523–530.
[6] J. Lavergne, J.M. Briantais, in: D.R. Ort, C.F. Yocum (Eds.), Oxygenic Photosynthesis: The Light Reactions, Kluwer Academic Publishing, Dordrecht, The Netherlands, 1996, pp. 265–287.
[7] E. Andreasson, P. Svensson, C. Weibull, P.-Å. Albertsson, Separation and characterisation of stroma and grana membranes—evidence for heterogeneity in antenna size of both photosystem I and photosystem II, Biochim. Biophys. Acta 936 (1988) 339–350.
[8] P. Svensson, E. Andreasson, P.-Å. Albertsson, Heterogeneity among photosystem I, Biochim. Biophys. Acta 1060 (1991) 45–50.
[9] F. Mamedov, H. Stefansson, P.-Å. Albertsson, S. Styring, Photosystem II in different parts of the thylakoid membrane: a functional comparison between different domains, Biochemistry 39 (2000) 10478–10486.
[10] L. Wollenberger, H. Stefansson, S.-G. Yu, P.-Å. Albertsson, Isolation and characterisation of vesicles originating from the chloroplast grana margins, Biochim. Biophys. Acta 1184 (1994) 93–102.
[11] B. Andersson, W. Haehnel, Location of photosystem I and photosystem II reaction centres in different thylakoid regions of stacked chloroplasts, FEBS Lett. 146 (1982) 13–17.
[12] T. Henrysson, C. Sundby, Characterization of photosystem II in stroma thylakoid membranes, Photosynth. Res. 25 (1990) 107–117.
[13] D.I. Arnon, Copper enzymes in isolated chloroplasts. Polyphenoloxidase in *Beta vulgaris*, Plant Physiol. 24 (1949) 1–15.
[14] R.J. Porra, W.A. Thompson, P.E. Kriedemann, Determination of accurate extinction coefficients and simultaneous equations for

assaying chlorophylls a and b extracted with four different solvents: verification of the concentration of chlorophyll standards by absorption spectroscopy, Biochim. Biophys. Acta 975 (1989) 384–394.
[15] W.C. Hoganson, G.T. Babcock, in: M. Sigel, A. Sigel (Eds.), Metal Ions in Biological Systems, Marcel Dekker, Basel, Switzerland, 1994, pp. 77–107.
[16] M. Rova, F. Mamedov, A. Magnuson, P.-O. Fredriksson, S. Styring, Coupled activation of the donor and the acceptor side of photosystem II during photoactivation of the oxygen evolving cluster, Biochemistry 37 (1998) 11039–11045.
[17] A.-F. Miller, G.W. Brudvig, A guide to electron paramagnetic resonance spectroscopy of photosystem II membranes, Biochim. Biophys. Acta 1056 (1991) 1–18.
[18] S. Styring, A.W. Rutherford, In the oxygen-evolving complex of photosystem II the S_0 state is oxidized to the S_1 state by D^+ (signal II slow), Biochemistry 26 (1987) 2401–2405.
[19] P.-Å. Albertsson, E. Andreasson, H. Stefansson, L. Wollenberger, Fractionation of the thylakoid membrane, Methods Enzymol. 228 (1994) 469–482.
[20] R.J.B. Debus, I.B.A. Sithole, G.T. Babcock, L. Mc Intosh, Directed mutagenesis indicates that the donor to $P680^+$ in photosystem II is tyrosine-161 of the D1 polypeptide, Biochemistry 27 (1988) 9071–9074.
[21] W.F.J. Vermaas, A.W. Rutherford, Ö. Hansson, Site-directed mutagenesis in photosystem II of the cyanobacterium Synechocystis sp. PCC 6803: donor D is a tyrosine residue in the D2 protein, Proc. Natl. Acad. Sci. U. S. A. 85 (1988) 8477–8481.
[22] G.T. Babcock, K. Sauer, Electron paramagnetic resonance signal II in spinach chloroplasts: 1. Kinetic analysis for untreated chloroplasts, Biochim. Biophys. Acta 325 (1973) 483–503.
[23] B.A. Diner, G.T. Babcock, in: D.R. Ort, C.F. Yocum (Eds.), Oxygenic Photosynthesis: The Light Reactions, Kluwer Academic Publishing, Dordrecht, The Netherlands, 1996, pp. 213–247.
[24] I. Vass, S. Styring, pH-dependent charge equilibria between tyrosine-D and the S-states in photosystem II. Estimation of relative midpoint redox potentials, Biochemistry 30 (1991) 830–839.
[25] C. Jegerschöld, S. Styring, Spectroscopic characterization of intermediate steps involved in donor-side-induced photoinhibition of photosystem II, Biochemistry 35 (1996) 7794–7801.
[26] S. Styring, I. Virgin, A. Ehrenberg, B. Andersson, Strong light photoinhibition of electron transport in photosystem II. Impairment of the function of the first quinone acceptor, Q_A, Biochim. Biophys. Acta 1015 (1990) 269–278.
[27] J.A.B. Weil, J.E.J.R. Wertz, Electron Paramagnetic Resonance, Wiley, New York, 1994.
[28] A. Melis, J.M. Andersson, Structural and functional organisation of the photosystems in spinach chloroplasts, antenna size, relative electron-transport capacity, and chlorophyll composition, Biochim. Biophys. Acta 724 (1983) 473–484.
[29] J.M. Anderson, A. Melis, Localisation of different photosystems in separate regions of chloroplast membrane, Proc. Natl. Acad. Sci. U. S. A. 80 (1983) 745–749.
[30] S.W. McCauley, A. Melis, Photosystem stoichiometry in higher plant chloroplasts, in: Progress in Photosyntesis Research, C. Sybesma (Ed.), Martinus Nijhoff, Dr. W. Junk Publishers, The Hague, The Netherlands, vol. II, 1987, pp. 245–248.
[31] W.S. Chow, A. Melis, J.M. Andersson, Adjustments of photosystem stoichiometry in chloroplasts improve the quantum efficiency of photosynthesis, Proc. Natl. Acad. Sci. U. S. A. 87 (1990) 7502–7506.
[32] W.S. Chow, A.B. Hope, J.M. Anderson, Oxygen per flash from leaf disks quantifies photosystem II, Biochim. Biophys. Acta 973 (1989) 105–108.
[33] J. Wihtmarsh, D.R. Ort, Stoichiometries of electron transport complexes in spinach chloroplasts, Arch. Biochem. Biophys. 231 (1984) 378–389.
[34] A. Melis, M. Spangfort, B. Andersson, Light absorption and electron-transport balance between photosystem II and photosystem I in spinach chloroplasts, Photochem. Photobiol. 45 (1987) 129–136.
[35] P. Jursinic, Photosystem II/I stoichiometry by the methods of absorbance change at 325 and 705 nm, 14C-Atrazine binding, and flash yields, in: Advances in Photosynthesis Research, C. Sybesma (Ed.), Martinus Nijhoff, Dr. W. Junk Publishers, The Hague, The Netherlands, 1984, vol. I, pp. 485–488.
[36] T. Hiyama, B. Ke, Difference spectra and extinction coefficients of $P700^+$, Biochim. Biophys. Acta 267 (1971) 160–171.
[37] E. Andreasson, P.-Å. Albertsson, Heterogeneity in photosystem I—the larger antenna of photosystem I is due to functional connection to a special pool of LHCII, Biochim. Biophys. Acta 1141 (1993) 175–182.
[38] P.-Å. Albertsson, E. Andreasson, P. Svensson, S.-G. Yu, Localization of cytochrome *f* in the thylakoid membrane: evidence for multiple domains, Biochim. Biophys. Acta 1098 (1991) 90–94.
[39] P.-Å. Albertsson, E. Andreasson, A. Persson, P. Svensson, Organisation of the thylakoid membrane with respect to the four photosystems, PSIα, PSIβ, PSIIα, and PSIIβ, in: M. Baltscheffsky (Ed.), Current Research in Photosynthesis, vol. II, Kluwer Academic Publishing, Dordrecht, The Netherlands, 1990, pp. 923–926.
[40] D.R. Ort, J. Whitmarsn, Inactive photosystem II centers: a resolution of discrepencies in photosystem II quantification, Photosynth. Res. 23 (1990) 101–104.
[41] S. Jansson, The light-harvesting chlorophyll *a*/*b*-binding proteins, Biochim. Biophys. Acta 1184 (1994) 1–19.
[42] N. Kamiya, J.-R. Shen, Crystal structure of oxygen-evolution photosystem II from *Thermosynechococcus vulcanus* at 3.7-Å resolution, Proc. Natl. Acad. Sci. U. S. A. 100 (2003) 98–103.
[43] A. Zouni, H.-T. Witt, J. Kern, P. Fromme, N. Krauss, W. Saenger, P. Orth, Crystal structure of photosystem II from *Synechococcus elongatus* at 3.8 Å resolution, Nature 409 (2001) 734–739.
[44] M.A. Harrison, A. Melis, Organization and stability of polypeptides associated with the chlorophyll A–B light-harvesting complex of photosystem II, Plant Cell Physiol. 33 (1992) 627–637.
[45] G.F. Peter, J.P. Thomber, Biochemical composition and organization of higher plant photosystem II light-harvesting pigment-proteins, J. Biol. Chem. 266 (1991) 16745–16754.
[46] G.F. Peter, J.P. Thornber, Biochemical evidence that the higher plant photosystem II core complex is organized as a dimer, Plant Cell Physiol. 32 (1991) 1237–1250.
[47] E.J. Boekema, J.F.L. van Breemen, H. van Roon, J.P. Dekker, Arrangement of photosystem II supercomplexes in crystalline macrodomains with in the thylakoid membrane of green plant chloroplasts, J. Mol. Biol. 301 (2000) 1123–1133.
[48] R.K. Juhler, E. Andreasson, S.-G. Yu, P.-Å. Albertsson, Composition of photosynthetic pigments in thylakoid membrane fractions from spinach, Photosynth. Res. 35 (1993) 171–178.
[49] C. Klughammer, U. Schreiber, An improved method, using saturating light pulses, for the determination of photosystem I quantum yield via $P700^+$ absorbance changes at 830 nm, Planta 192 (1994) 261–268.
[50] R. Delsome, Wavelength dependence of the quantum yield of charge separation in photosynthesis: photoacoustic study of light energy distribution among various pigment complexes, Isr. J. Chem. 38 (1998) 237–246.